engineering proceedings

MDPI

Proceeding Paper

Water-Evaporation Supported Fuel-Cell Cooling Architectures for Aircraft †

Raphael Gebhart [1,*], Luis Weber [2] and Franciscus L. J. van der Linden [1]

[1] German Aerospace Center (DLR), Münchener Straße 20, 82234 Weßling, Germany
[2] Faculty of Mechanical Engineering, Ostbayerische Technische Hochschule Regensburg, Seybothstraße 2, 93053 Regensburg, Germany
* Correspondence: raphael.gebhart@dlr.de
† Presented at the 15th EASN International Conference, Madrid, Spain, 14–17 October 2025.

Abstract

The thermal management-induced drag of conventional ram-air cooling systems for low-temperature fuel-cell propulsion can account for roughly 20% to 25% of total drag in fuel-cell aircraft concepts, while its mass and power impact at the overall aircraft level are far less significant. This drag penalty can severely reduce efficiency, especially when additional parallel power sources for takeoff such as gas turbine engines are undesirable. To address this, we propose augmenting low- and medium-temperature fuel-cell cooling with an auxiliary water-evaporation system. This mechanism is used only when needed, primarily during takeoff in hot ambient conditions, while the ram-air system can be downsized to meet cruise requirements. Water evaporation can achieve coefficients of performance of 50 to 100, while reducing the required mass flow by two orders of magnitude. It provides a heat-rejection energy density of approximately 670 Wh/kg, far exceeding that of state-of-the-art high-power-density batteries. Furthermore, the resulting vapor can be vented overboard, and the system is expected to outperform batteries in reliability, durability, and environmental impact. The paper introduces several architectures for integrating water-evaporation cooling into aircraft systems and discusses their respective advantages, limitations, and implications for overall aircraft performance. Initial results indicate that enabling evaporative cooling can significantly reduce the required ram-air channel size and drag, offering a promising pathway to more efficient fuel-cell-powered aircraft. In the EU project TheMa4HERA, aircraft-level design trades and scaled experimental validation for aviation applications of water evaporation are planned in 2026.

Keywords: fuel-cell aircraft; thermal management; evaporative cooling; cooling architectures; ram-air cooling; boost system

Academic Editors: Spiros Pantelakis, Andreas Strohmayer and Gustavo Alonso

Published: 13 May 2026

1. Introduction

Hydrogen fuel-cell propulsion is a promising pathway toward climate-compatible aviation, but it introduces a severe thermal-management bottleneck at aircraft scale. Low-temperature polymer electrolyte membrane (PEM) fuel cells convert roughly half of the reaction enthalpy into electric work, leaving a comparable amount as waste heat that must be rejected at temperatures as low as 80 °C [1–3]. This is because PEM fuel cells must typically operate below the saturation temperature of liquid water at stack pressure, although efforts aim to increase the operating temperature as much as possible. At power levels above a few kilowatts, air cooling becomes impractical; the state of the art therefore relies

on a closed-loop liquid coolant cycle feeding a ram-air heat exchanger [2]. Ram-air heat exchangers perform well during cruise but become highly constrained during takeoff due to high ambient temperatures, high power demand, and low aircraft speed. Consequently, they must be sized for a worst-case takeoff condition, imposing significant drag penalties throughout the mission [3,4]. In representative studies, thermal management system (TMS)-induced drag accounts for roughly 20% to 25% of the total drag in fuel-cell aircraft concepts [3]. Figure 1a shows a Sankey diagram for a fuel-cell powertrain. Rough estimates of 50% fuel-cell efficiency, 95% powertrain efficiency, 85% propeller efficiency, and 25% TMS-induced drag for fuel-cell cooling are assumed. Thus, TMS-induced drag reduces the overall propulsive efficiency from 40% to 30%. Furthermore, the oversizing problem scales unfavorably with propulsion power and thus limits the viability of commercial-class fuel-cell aircraft.

To address this constraint, this paper proposes adding an on-demand evaporation path using water as coolant in an open-loop system. The key idea is to keep the conventional, fuel-cell-compatible cooling loop unchanged and support it during short high-load phases through water evaporation.

We develop and compare several architectures for implementing this concept. Their impact at overall aircraft level in terms of mass, drag and power consumption will be assessed as part of the EU project TheMa4HERA in 2026.

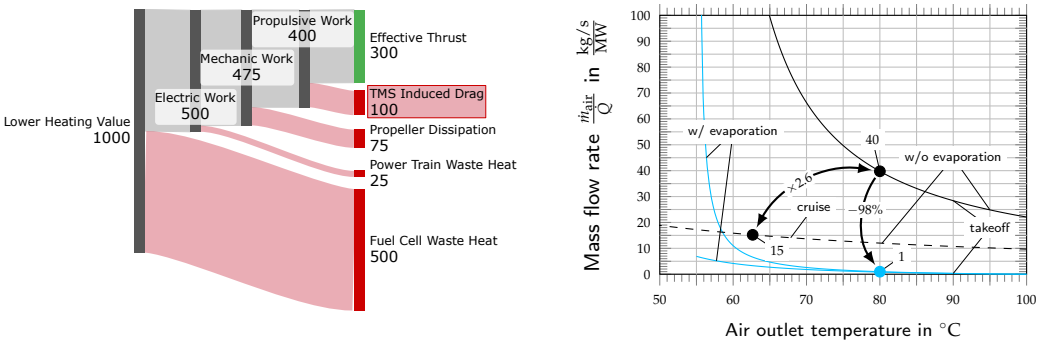

(**a**) (**b**)

Figure 1. (**a**) Sankey diagram (created with SankeyMATIC); Colors indicate energy type: grey for work transfer, green for useful thrust and red for losses; Line width scales with energy magnitude and nodes indicate conversion stages; (**b**) Air mass flow rates $\dot{m}_{\mathrm{air}}$ per heat flow rate $\dot{Q}$. Takeoff is $\Delta T_{\mathrm{ISA}} = 40\,\mathrm{K}$, cruise $\Delta T_{\mathrm{ISA}} = 20\,\mathrm{K}$ at flight level FL250 (25 000 ft = 7620 m), true air speed 300 KTAS $\approx 154\,\mathrm{m/s}$); ambient relative humidity $\mathrm{RH}_\infty = 100\%$.

2. State of the Art and Problem Formulation

2.1. Scaling of Air-Cooled Waste Heat Rejection

Assuming an ambient temperature of $\Delta T_{\mathrm{ISA}} = 40\,\mathrm{K}$ (temperature difference to the International Standard Atmosphere (ISA), $T_\infty = 55\,^\circ\mathrm{C}$) and a heat-exchanger outlet air temperature of $T_{\mathrm{out}} = 80\,^\circ\mathrm{C}$, the required air mass flow $\dot{m}_{\mathrm{air}}$ per waste heat $\dot{Q}$ is

$$\frac{\dot{m}_{\mathrm{air}}}{\dot{Q}} = \frac{1}{c_{p,\mathrm{air}}(T_{\mathrm{out}} - T_\infty)} = \frac{40\,\mathrm{kg/s}}{\mathrm{MW}}, \tag{1}$$

where $c_{p,\mathrm{air}}$ is the specific heat capacity of air at constant pressure. A megawatt-class fuel-cell system therefore requires several hundred kilograms per second of cooling air under hot-day takeoff conditions, comparable to the mass flow rates of turbofan engines.

Accordingly, the ram-air fans for fuel-cell cooling are similar in size to aircraft propellers. Furthermore, unlike turbofan bypass air, which provides the main thrust contribu-

tion, the fuel-cell cooling air must pass through a heat exchanger, where it likely loses a significant portion of its total pressure. Concepts exist to mitigate TMS-induced drag by exploiting fuel-cell waste heat via the Meredith effect, which can provide benefits during cruise [5]. However, this further complicates cooling during takeoff and necessitates an alternative solution for this phase.

The TMS-induced drag creates a snowball effect: additional thrust is required to offset the drag, increasing required power, fuel-cell waste heat, cooling mass flow rate, and consequently the drag. This can amount to approximately 20% to 25% of takeoff power, which appears unacceptable from an aircraft-level efficiency and sizing perspective.

An air outlet temperature of $T_{\text{out}} = 80\,^{\circ}\text{C}$ corresponds to a fuel-cell temperature $T_{\text{FC}} \approx 90\,^{\circ}\text{C}$ at a heat-exchanger efficiency of roughly 70%. Assuming the same heat-exchanger efficiency during cruise at flight level FL250 (25,000 ft = 7620 m), 300 KTAS (knots true airspeed, approximately 154 m/s), and $\Delta T_{\text{ISA}} = 20\,\text{K}$, the required cooling air mass flow rate is $\dot{m}_{\text{air}} = 15\,\text{kg/s}$ per MW of heat. Thus, during cruise the air mass flow rate decreases by a factor of 2.6 if takeoff and cruise power delivered by the fuel cell are identical; see Figure 1b. Since takeoff power typically exceeds cruise power, the oversizing is expected to be even more severe, for example, by a factor of $2 \times 2.6 \approx 5$.

2.2. Existing Evaporative Concepts and Limitations for Aviation

Evaporative cooling of PEM fuel cells has been demonstrated, typically via direct water injection into the anode or cathode channels [6–8]. Placing evaporation close to the reaction sites minimizes heat-transfer losses and can yield an "optimal" system; however, high water purity is required and the risk of flooding must be carefully managed.

Kösters et al. (2022) [9] proposed a water-based heat-pump system that evaporates water in the fuel-cell cooling channels; see Figure 2a. While this avoids flooding, it violates the usual pressure hierarchy of coolant > anode > cathode required to ensure desired leak-flow directions [10]. Nevertheless, heat pumps are in principle feasible, either by changing the heat-transfer medium or by coupling to a conventional cooling loop. Their main limitation is the snowball effect caused by the required compressor power.

From energy conservation,

$$\begin{aligned} \Delta\dot{H}_{\text{reaction}} &= P + \dot{Q}_{\text{evap}}\,, & P &= \eta\Delta\dot{H}_{\text{reaction}}\,, & P &= P_{\text{prop}} + P_{\text{CMP}}\,, \\ \dot{Q}_{\text{cond}} &= \dot{Q}_{\text{evap}} + P_{\text{CMP}}\,, & \dot{Q}_{\text{evap}} &= \text{COP}P_{\text{CMP}}\,, & \dot{Q}_{\text{cond}} &= \dot{m}_{\text{air}}c_{p,\text{air}}\Delta T\,, \end{aligned} \tag{2}$$

the ram-air flow requirement becomes

$$\frac{\dot{m}c_{p,\text{air}}}{P_{\text{prop}}} = \frac{\beta}{\Delta T}, \quad \beta = \alpha\frac{1+\text{COP}}{\text{COP}-\alpha}, \quad \alpha = \frac{1-\eta}{\eta}\,, \tag{3}$$

where $\Delta\dot{H}_{\text{reaction}}$ is the reaction enthalpy flow rate, P is power, η is efficiency, COP is the coefficient of performance, α is the ratio of fuel-cell waste heat to fuel-cell power, and β is the ram-air heat-scaling factor. Subscripts denote $(\bullet)_{\text{CMP}}$ compressor, $(\bullet)_{\text{evap}}$ evaporator, $(\bullet)_{\text{cond}}$ condenser, and $(\bullet)_{\text{prop}}$ propulsive quantities. Note, that neglecting the snowball effect, i.e., replacing the third equation with $P = P_{\text{prop}}$, leads to $\beta = \alpha(1 + 1/\text{COP})$.

An advantage of integrating a heat pump, is the increase in air temperature difference, ΔT, resulting from an elevated heat exchanger (condenser) temperature. However, it simultaneously increases the waste heat to be dissipated, represented by β.

For an efficiency of $\eta = 0.5$, one obtains $\alpha = 1$ and $\beta = 1 + 2/(\text{COP} - 1)$. Figure 2b illustrates the resulting increase in ram-air heat flow, $\Delta\dot{Q}_{\text{cond}} \sim \beta - 1$, as a function of COP for $\eta = 0.5$. Two effects become evident. First, each watt of compressor power requires rejection of two additional watts of heat: one from the compressor itself and one from the

associated increase in fuel-cell waste heat. Second, for typical heat-pump coefficients of performance COP = 2 to 3, the snowball effect is already pronounced.

For example, at COP = 2, the additional heat load increases from 50% without the snowball effect to 100% when accounting for the primary effect, and further to 200% when the snowball effect is included; see Figure 2b. It is unlikely that the heat pump can proportionally increase the attainable temperature rise ΔT (by a factor of three). Therefore, the required ram-air mass flow and associated heat-exchanger frontal area are likely to exceed those of a system without a heat pump, while also adding weight, cost, and complexity.

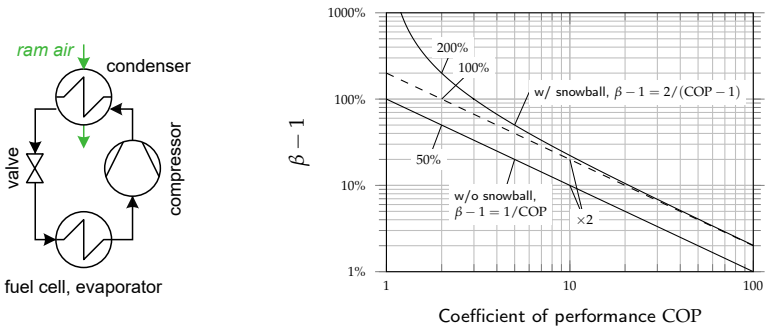

(**a**) (**b**)

Figure 2. (**a**) Heat pump schematic; (**b**) Increase in ram-air heat flow rate $\Delta\dot{Q}_{\mathrm{cond}} \sim \beta - 1$ depending on the system coefficient of performance COP.

3. Water-Evaporation Supported Hybrid Cooling Concept

We propose a hybrid architecture, shown in Figure 3a, consisting of: (1) a conventional closed cooling loop (liquid, e.g., ethylene glycol water (EGW), or two-phase, e.g., methanol) for heat transport that satisfies strict fuel-cell requirements such as high purity, limited electrical conductivity, and freeze protection; (2) a conventional ram-air cooling system for heat dissipation, optimized for cruise; and (3) an additional open-loop water-evaporation cooling system to provide support during high-demand phases, e.g., takeoff under hot ambient conditions. The water vapor is vented overboard. This arrangement satisfies fuel-cell constraints (purity, conductivity, pressure hierarchy) while providing a powerful transient heat sink.

Water evaporation exploits latent heat and favorable thermophysical properties. Assuming the same environmental conditions as for air cooling (Equation (1)) yields

$$\frac{\dot{m}_{\mathrm{H_2O}}}{\dot{Q}} = \frac{1}{\Delta h_{\mathrm{vap}}(T_0) + c_{p,\mathrm{v}}(T_{\mathrm{out}} - T_0) - c_{\mathrm{w}}(T_\infty - T_0)} = 0.41\frac{\mathrm{kg/s}}{\mathrm{MW}} \approx 1\,\%\frac{\dot{m}_{\mathrm{air}}}{\dot{Q}}, \qquad (4)$$

where $T_0 = 0\,^\circ\mathrm{C}$ is the reference temperature, $\Delta h_{\mathrm{vap}}(T_0) \approx 2.50\,\mathrm{MJ/kg}$ is the latent heat of evaporation, $c_{\mathrm{w}} \approx 4.19\,\mathrm{kJ/(kg\,K)}$ is the specific heat capacity of liquid water, and $c_{p,\mathrm{v}} \approx 1.86\,\mathrm{kJ/(kg\,K)}$ is the specific heat capacity of water vapor at constant pressure.

Under these conditions, the required water mass flow is about two orders of magnitude lower than the required air mass flow. Crucially, only the amount of water needed for the time-limited boost (minutes) must be carried, and venting the vapor discards the mass afterward.

A 5 min boost absorbing 50% of the total heat load therefore requires about 62 kg of evaporated water per MW. For the given ambient conditions, water evaporation provides an energy density of about 670 Wh/kg. Although batteries with C-rates of about 10 exist, their cell-level energy density is currently below 100 Wh/kg [11]. Therefore, the water-evaporation system is expected to be lighter than a battery-based alternative.

https://doi.org/10.3390/engproc2026133145

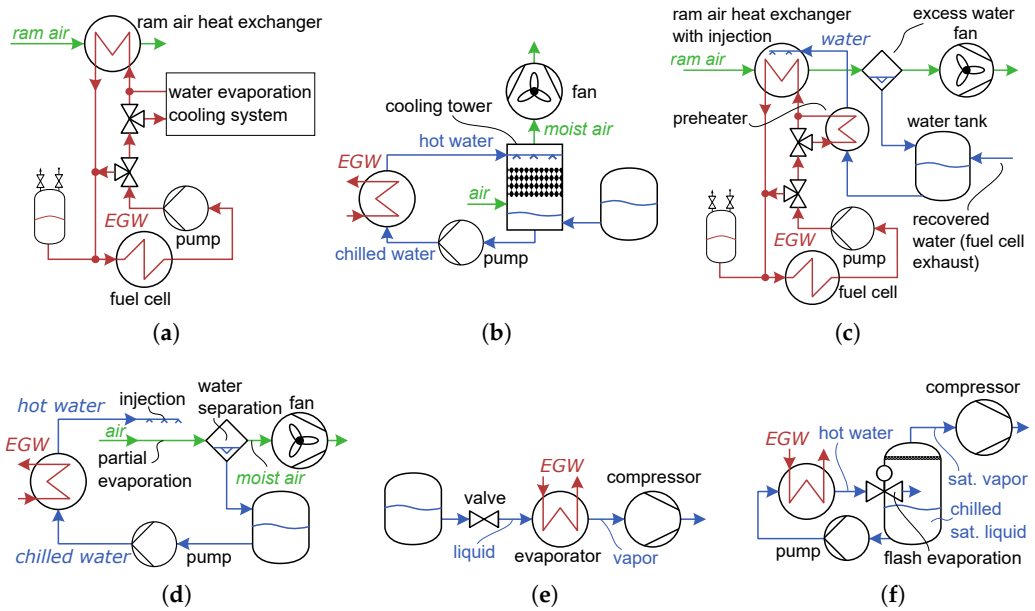

Figure 3. (**a**) Hybrid cooling concept: conventional closed loop ethylene glycol–water (EGW) stack cooling plus on-demand open loop water-evaporation support used only during high cooling demand; (**b**) Counter flow cooling tower with fill material; (**c**) Water injection on ram-air heat exchanger including optional preheating and recovery of excess water; (**d**) Parallel flow cooling tower using droplets and a water separator; (**e**) Open-loop reduced-pressure high-temperature heat pump; (**f**) Flash evaporation.

4. Architecture Options for Implementing Water-Evaporation Support

4.1. Water Injection on Ram-Air Heat Exchanger

Figure 3 shows simplified schematics of architecture options for implementing water-evaporation support. The minimal modification to conventional ram-air cooling is to inject water so that it evaporates within the airstream, effectively implementing spray cooling as shown in Figure 3c. Spray cooling can achieve high local heat-flux removal, typically 100 kW/m^2 to 500 kW/m^2, depending on droplet size, velocity, and surface conditions [12]. Heat is transferred through droplet impingement, thin-film evaporation, and secondary nucleate boiling, with droplet diameters of 50 µm to 300 µm generally providing a good compromise between evaporation efficiency and surface coverage. At low superheats (<20 K to 30 K), single-phase forced convection dominates; at higher wall superheats, nucleate boiling and thin-film evaporation significantly enhance heat removal. Efficiency decreases if flooding or vapor films (Leidenfrost effect) occur, highlighting the need to control droplet distribution and residence time.

For a ram-air heat exchanger, even a small water spray can markedly enhance cooling if droplet size, velocity, and residence time are optimized. However, excessive water may reduce evaporation efficiency, especially in heat exchangers not designed for wet operation. Preheating the liquid and recovering excess water, as shown in Figure 3c, can mitigate these effects and improve overall performance, representing an intermediate step toward a cooling-tower system; see Figure 3b.

The moisture uptake of air is limited by the vapor pressure curve of water; see Figure 4a. At a given temperature, it defines the maximum vapor partial pressure and thus the maximum molar and mass fractions of vapor in air.

Figure 1b shows the required air mass flow $\dot{m}_{air}$ as a function of outlet temperature T_{out}, assuming saturated outlet conditions. At 80 °C, the required air mass flow decreases to approximately 1 kg/s, a reduction of about 98% compared to dry cooling.

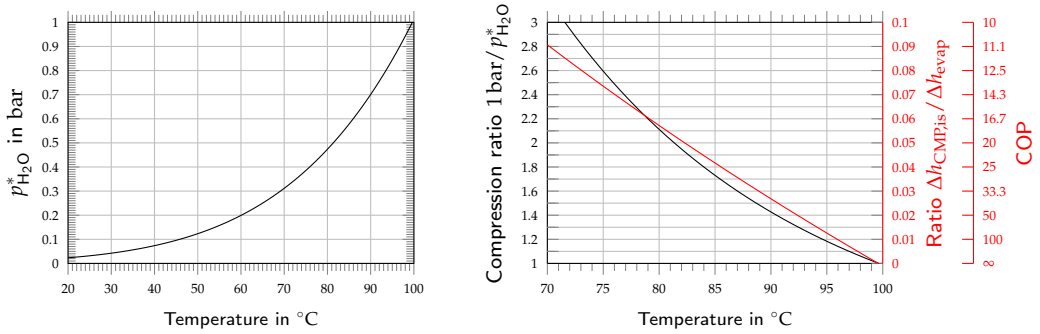

(**a**) (**b**)

Figure 4. (**a**) Vapor pressure chart of water; (**b**) Evaporation performance: Compression ratio (black curve, left y-axis) and theoretical coefficient of performance COP (red curve, right y-axis) of reduced-pressure evaporation depending on the evaporation temperature; $p^*_{H_2O}$ is the vapor pressure of water, Δh_{evap} is the enthalpy difference of evaporation, and $\Delta h_{CMP,is}$ is the compressor isentropic specific work.

Figure 1b also shows that ambient relative humidity RH_∞ significantly affects the air mass flow at low outlet temperatures ($T_{out} < 60\,°C$), whereas its influence becomes negligible at higher outlet temperatures ($T_{out} > 70\,°C$) due to the exponential vapor-pressure curve in Figure 4a, which renders inlet moisture negligible.

Commonly only a small fraction of the heat is absorbed as sensible heat, leaving the water mass flow nearly independent of outlet temperature. However, typical ram-air velocities may be too high to allow effective evaporation.

4.2. Cooling Tower Principle

To decouple cruise ram-air requirements from takeoff evaporation, water can be evaporated in a dedicated subsystem, as illustrated in Figure 3a. Cooling towers are widely used in stationary applications. Although transferring such systems directly to aircraft is impractical, the underlying physical principles are likely transferable; see Figure 3b,d. In a cooling tower, hot water partially evaporates into an airstream, cooling the liquid while heating and humidifying the air [13]. Ideally, the air exits saturated at the water-inlet temperature, enabling substantially higher moisture uptake due to the exponential saturation vapor-pressure curve; see Figure 4a. Similarly, the water temperature can approach the ambient wet-bulb temperature, which may be significantly below the dry-bulb temperature. The cooled water is then recirculated to the heat source.

Cooling towers involve two processes: (i) heat and mass transfer between water and air and (ii) recovery of the cooled water. Heat transfer can be enhanced using fill media (Figure 3b), which increase residence time and surface area, or by atomizing the water into fine droplets (Figure 3d). A wide range of fill- and droplet-based configurations exists [14]. Flow arrangements include counterflow (Figure 3b), crossflow, and parallel flow (Figure 3d), with counterflow generally providing the highest thermal effectiveness. For aircraft applications, the airflow would be fan-driven, allowing substantially smaller installations than natural-draft cooling towers, where buoyancy induces the flow. Water recovery in conventional towers is gravity-driven (Figure 3b). For droplet-based airborne systems, however, an additional separator may be advantageous (Figure 3d). Smaller droplets enhance heat transfer but are harder to recover, implying the existence of an optimal droplet size.

Conventional cooling towers operate with water inlet temperatures as low as 30 °C and are typically designed to approach the ambient wet-bulb temperature to maximize

power-plant efficiency. In contrast, fuel-cell systems supply water near 100 °C, substantially increasing evaporative potential.

Sensible heat transfer and evaporation are usually separated, although integration of a heat exchanger into the cooling tower is possible. The water reservoir can be integrated into the tower (Figure 3d) or separated from it (Figure 3b). However, efficient evaporation into air requires relatively long residence times, i.e., low air velocities, leading to installations that are likely too large for aircraft applications.

4.3. Reduced-Pressure Evaporation

The saturation temperature of liquid water depends on pressure, as shown in Figure 4a. If the fuel-cell temperature is below 100 °C, the evaporation pressure must therefore be reduced relative to ambient conditions.

This can be achieved using a compressor and a valve, as illustrated in Figure 3e, which together control both the mass flow rate and the pressure in the evaporator. The evaporator could also be integrated directly into the water reservoir, in which case the valve may not be required. A phase separator downstream of the heat exchanger and recirculation of saturated liquid water are likewise possible to reduce the required supersaturation of steam at the compressor inlet.

The resulting configuration corresponds to an open-loop, reduced-pressure, high-temperature heat pump (HTHP) using water (R718) as the working fluid [15,16]. The environment acts as the condenser, and the loop is effectively closed whenever the reservoir is refilled with liquid water.

Canders et al. (2019) [17] proposed a similar system to boost electric-system cooling. However, his application required temperatures as low as 40 °C, demanding compression ratios as high as 13.5. This necessitates a multistage radial compressor and yields a theoretical coefficient of performance of 3.6. For fuel-cell cooling, such a configuration would already trigger a severe snowball effect (see Figure 2b), making it impractical.

At higher temperatures, the required compression ratios become far more manageable, as shown in Figure 4b. This results in theoretical coefficients of performance of approximately 20 at 82 °C, 50 at 91 °C, and 100 at 96 °C evaporation temperature. These values highlight the strong temperature dependence of system performance and underscore the importance of minimizing heat-transfer losses and increasing the fuel-cell temperature.

At low compression ratios, a fan and diffuser or a jet pump driven by conventional ram air may suffice to achieve the required compression ratio.

4.4. Flash Evaporation

Flash evaporation occurs when a liquid experiences a sudden pressure drop below its saturation pressure, causing a portion to evaporate almost instantaneously [18]. In this setup, hot water expands through a throttling valve, producing a mixture of saturated vapor and liquid at reduced pressure and temperature. The vapor is extracted by a compressor, while the remaining liquid is recirculated and reheated, as shown in Figure 3f.

Flash evaporation reverses the sequence of heat transfer and expansion compared to reduced-pressure evaporation (Figure 3e), allowing the heat exchanger to operate above ambient pressure. As noted by Mansour and Müller (2019) [18], flash evaporation is highly sensitive to inlet temperature, pressure drop, and liquid superheat, and only a fraction of the liquid can be vaporized. For the present application, flash evaporation is expected to yield lower heat-transfer coefficients and lower specific heat flow likely making it less efficient than reduced-pressure evaporation.

https://doi.org/10.3390/engproc2026133145

4.5. Elevated Temperatures

If stacks operate above 100 °C, evaporation can occur above ambient pressure. Pressurized vapor could then be expanded through a turbine or nozzle to generate work or thrust. As conventional ram-air cooling also becomes easier at higher stack temperatures, water-evaporation-assisted fuel-cell cooling is expected to be most competitive when the fuel-cell temperature lies in the range of about 90 °C to 150 °C.

At even higher operating temperatures, or under lower ambient conditions, extracting useful work from the fuel-cell waste heat becomes increasingly attractive, either via the Meredith effect [5], coupling to an organic Rankine cycle [19], or integrating with a gas turbine in the case of a solid oxide fuel cell operating e.g., at 1000 °C [20,21]. This demonstrates that variations in stack temperature are the primary driver of changes in the optimal system when considering mass, drag, power, complexity, and cost at the overall aircraft level.

5. Conclusions

PEM fuel-cell propulsion at aviation scale is dominated by takeoff cooling constraints, which require large ram-air systems and increase cruise drag.

Water-evaporation-supported hybrid cooling, leveraging latent heat, can temporary reduce air mass flow by two orders of magnitude, allowing ram-air systems to be optimized for cruise, thus reducing overall drag and potentially mass.

Among feasible architectures, simple water injection on existing heat exchangers offers the most practical path, but evaporation demands may not match conventional ram-air design. Dedicated water-evaporation systems, such as reduced-pressure evaporation, may have a significantly greater impact on cooling performance.

In TheMa4HERA, aircraft-level design trades and scaled experimental validation for aviation applications are planned in 2026. These will assess mass, drag, and power demand and compare evaporation-supported hybrid cooling with conventional cooling and battery support during takeoff.

Author Contributions: Conceptualization, R.G.; methodology, R.G.; software, R.G. and L.W.; validation, R.G. and L.W.; formal analysis, R.G. and L.W.; investigation, R.G. and L.W.; resources, R.G.; data curation, R.G. and L.W.; writing—original draft preparation, R.G.; writing—review and editing, R.G. and F.L.J.v.d.L.; visualization, R.G.; supervision, R.G.; project administration, F.L.J.v.d.L.; funding acquisition, F.L.J.v.d.L. All authors have read and agreed to the published version of the manuscript.

Funding: This work was carried out as part of the European project TheMa4HERA. The project is supported by the Clean Aviation Joint Undertaking and its members, and funded by the European Union under Grant Agreement No. 101102008.

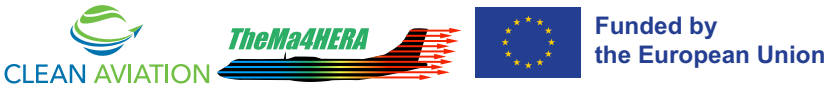

Institutional Review Board Statement: Not applicable.

Informed Consent Statement: Not applicable.

Data Availability Statement: Data belongs to the TheMa4HERA project under Grant Agreement No. 101102008 and cannot be shared without explicit consent of the consortium.

Conflicts of Interest: The authors declare no conflicts of interest.

References

1. Asli, M.; König, P.; Sharma, D.; Pontika, E.; Huete, J.; Konda, K.R.; Mathiazhagan, A.; Xie, T.; Höschler, K.; Laskaridis, P. Thermal management challenges in hybrid-electric propulsion aircraft. *Prog. Aerosp. Sci.* **2024**, *144*, 100967. [CrossRef]

2. van Heerden, A.; Judt, D.; Jafari, S.; Lawson, C.; Nikolaidis, T.; Bosak, D. Aircraft thermal management: Practices, technology, system architectures, future challenges, and opportunities. *Prog. Aerosp. Sci.* **2022**, *128*, 100767. [CrossRef]
3. Schröder, M.; Becker, F.; Gentner, C. Optimal design of proton exchange membrane fuel cell systems for regional aircraft. *Energy Convers. Manag.* **2024**, *308*, 118338. [CrossRef]
4. Schröder, M.; Becker, F.; Kallo, J.; Gentner, C. Optimal operating conditions of PEM fuel cells in commercial aircraft. *Int. J. Hydrogen Energy* **2021**, *46*, 33218–33240. [CrossRef]
5. Frey, A.C.; Stonham, J.; Bosak, D.; Sangan, C.M.; Pountney, O.J. Radiators in fuel cell powered aircraft: The effect of heat rejection on drag. *Appl. Therm. Eng.* **2025**, *274*, 126697. [CrossRef]
6. Cochet, M.; Forner-Cuenca, A.; Manzi-Orezzoli, V.; Siegwart, M.; Scheuble, D.; Boillat, P. Enabling High Power Density Fuel Cells by Evaporative Cooling with Advanced Porous Media. *J. Electrochem. Soc.* **2020**, *167*, 084518. [CrossRef]
7. Fly, A.; Thring, R. A comparison of evaporative and liquid cooling methods for 0 vehicles. *Int. J. Hydrogen Energy* **2016**, *41*, 14217–14229. [CrossRef]
8. Striednig, M.; Mularczyk, A.; Liu, W.; Scheuble, D.; Cochet, M.; Boillat, P.; Schmidt, T.J.; Büchi, F.N. Evaporative cooling for polymer electrolyte fuel cells - An operando analysis at technical single cell level. *J. Power Sources* **2023**, *556*, 232419. [CrossRef]
9. Kösters, T.L.; Liu, X.; Kožulović, D.; Wang, S.; Friedrichs, J.; Gao, X. Comparison of phase-change-heat-pump cooling and liquid cooling for PEM fuel cells for MW-level aviation propulsion. *Int. J. Hydrogen Energy* **2022**, *47*, 29399–29412. [CrossRef]
10. Li, Y.; Zhao, X.; Tao, S.; Li, Q.; Chen, W. Experimental Study on Anode and Cathode Pressure Difference Control and Effects in a Proton Exchange Membrane Fuel Cell System. *Energy Technol.* **2015**, *3*, 946–954. [CrossRef]
11. Corporation, T. SCiB™ Rechargeable Lithium-Titanate (LTO) Battery Brochure. 2025. Available online: https://www.global.toshiba/content/dam/toshiba/ww/products-solutions/battery/scib/pdf/ToshibaRechargeableBattery-en.pdf (accessed on 27 March 2026).
12. Kim, J. Spray cooling heat transfer: The state of the art. *Int. J. Heat Fluid Flow* **2007**, *28*, 753–767. [CrossRef]
13. Mohiuddin, A.; Kant, K. Knowledge base for the systematic design of wet cooling towers. Part I: Selection and tower characteristics. *Int. J. Refrig.* **1996**, *19*, 43–51. [CrossRef]
14. Erens, P.J.; Reuter, H.C.R., N4 Kühltürme. In *VDI-Wärmeatlas*; Springer: Berlin/Heidelberg, Germany, 2013; pp. 1655–1674. [CrossRef]
15. Arpagaus, C.; Bless, F.; Uhlmann, M.; Schiffmann, J.; Bertsch, S.S. High temperature heat pumps: Market overview, state of the art, research status, refrigerants, and application potentials. *Energy* **2018**, *152*, 985–1010. [CrossRef]
16. Hamid, K.; Sajjad, U.; Ulrich Ahrens, M.; Ren, S.; Ganesan, P.; Tolstorebrov, I.; Arshad, A.; Said, Z.; Hafner, A.; Wang, C.C.; et al. Potential evaluation of integrated high temperature heat pumps: A review of recent advances. *Appl. Therm. Eng.* **2023**, *230*, 120720. [CrossRef]
17. Canders, W.R.; Hoffmann, J.; Henke, M. Cooling Technologies for High Power Density Electrical Machines for Aviation Applications. *Energies* **2019**, *12*, 4579. [CrossRef]
18. Mansour, A.; Müller, N. A review of flash evaporation phenomena and resulting shock waves. *Exp. Therm. Fluid Sci.* **2019**, *107*, 146–168. [CrossRef]
19. Rahbar, K.; Mahmoud, S.; Al-Dadah, R.K.; Moazami, N.; Mirhadizadeh, S.A. Review of organic Rankine cycle for small-scale applications. *Energy Convers. Manag.* **2017**, *134*, 135–155. [CrossRef]
20. Singh, M.; Zappa, D.; Comini, E. Solid oxide fuel cell: Decade of progress, future perspectives and challenges. *Int. J. Hydrogen Energy* **2021**, *46*, 27643–27674. [CrossRef]
21. Dotzauer, N. Control Scheme of a Solid Oxide Fuel Cell System for Regional Aircraft. In Proceedings of the AIAA SCITECH 2025 Forum, Orlando, FL, USA, 6–10 January 2025. [CrossRef]